J. Fluid Mech. (1986), *vol.* 171, *pp.* 309–338
Printed in Great Britain

Shear-wave speeds and elastic moduli for different liquids. Part 2. Experiments

By D. D. JOSEPH, O. RICCIUS AND M. ARNEY

Department of Aerospace Engineering and Mechanics,
University of Minnesota, Minneapolis, MN 55455, USA

(Received 25 March 1985 and in revised form 21 March 1986)

In this paper we describe the experimental apparatus that we use to measure transit speeds. Tables of measured values of transit speeds and the corresponding values of the shear modulus are presented. The criteria we use to determine if a transit speed is a shear-wave speed are described and applied to the data. The main criteria are that transit speeds should be independent of the gap size and the corresponding value of the shear modulus should be consistent with independent rheometrical measurements. All the elastic liquids and many liquids that are usually assumed to be Newtonian satisfy our criteria for shear waves. We present evidence that the measured wave speeds are associated with slower-relaxing molecular structures in the liquids.

1. The wave-speed meter

The wave-speed meter utilizes a Couette apparatus with coaxial cylinders which may rotate independently. The radius of the outer cylinder is b and that of the inner cylinder is a; $b-a=d$ is the gap size. Liquid of height L is placed in the gap. The outer cylinder is moved impulsively. A shear wave propagates into the interior, toward the cylinder at $r=a$. After a certain time, the transit time, the inner cylinder is set into motion. The transit time would be the time of first reflection if the fluid was elastic or the diffusion time if the fluid was inelastic (Newtonian). We say that the fluid is elastic if the transit time is proportional to the gap size, with the same constant of proportionality for all sufficiently small gap sizes. The reciprocal of this constant is the wave speed.

1.1. *The apparatus*

A sketch of our wave-speed apparatus is shown in figures 1 and 2. A rigid structure is mounted on a heavy metal table, which supports the moving parts of the apparatus. The rigid structure consists of the upper (C) and lower (D) plates and three supporting pillars. The outer cylinder (A) is suspended on open ball bearings lying in grooves on the lower and upper plates, see figure 2. The inner cylinder (B) is designed to rotate easily. It is mounted on conical points which rest in pivot bearings, see figure 2. The inner cylinders that we use have very low moments of inertia. The frictional resistance to the motion of the inner cylinder is negligible. The test liquids are pushed into the gap between the cylinders by a plunger in a cylinder shown in figure 3. The fluid enters the gap through the lower bearing. This method of loading suppresses the formation of air bubbles in the test liquid. The inner cylinder is buoyed up by the liquid. It is seated properly in the bottom pivot bearing by adding an appropriate weight on the top of the upper bearing. This weight is evident in figures 1 and 3.

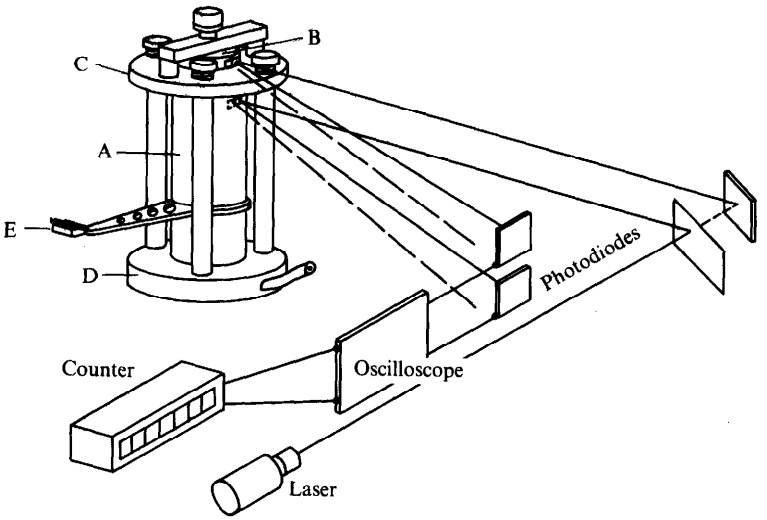

FIGURE 1. Sketch of the wave-speed meter.

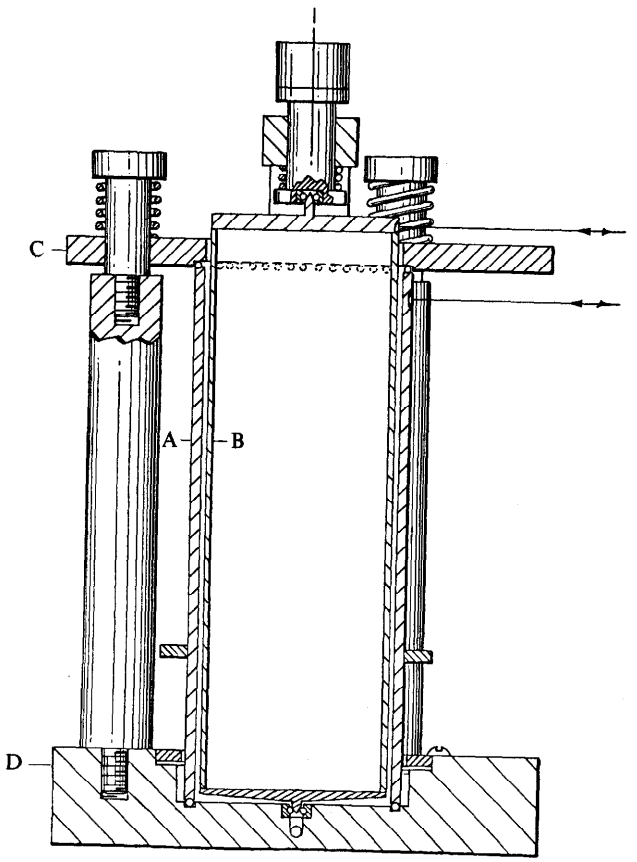

FIGURE 2. Details of the cylinders' assembly.

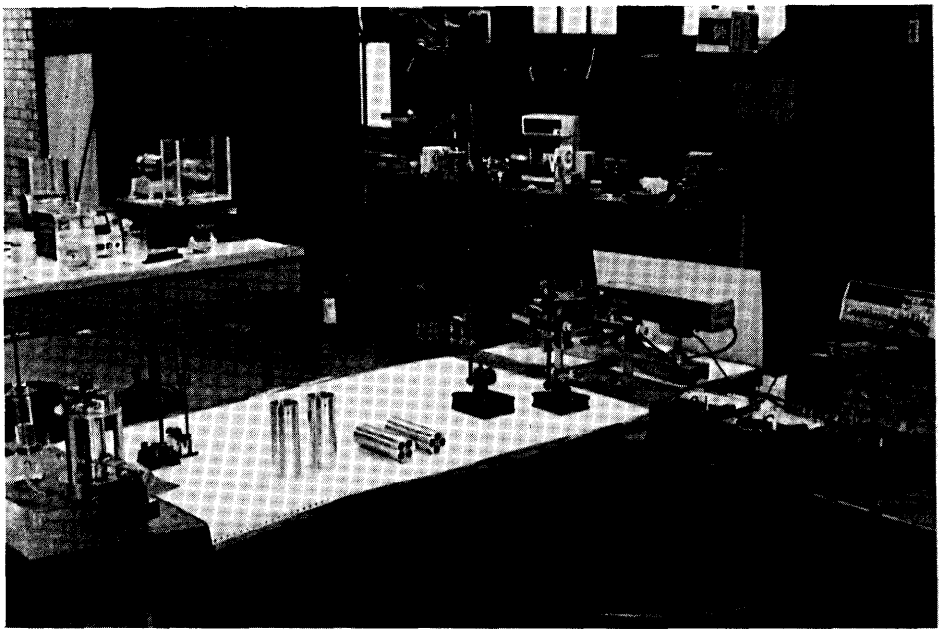

FIGURE 3. Photograph of the wave-speed meter.

1.2. *Measurements of transit times*

A transit-time measurement is started by applying an impulsive force to the outer cylinder with a simple kicking device. To do this, a spring-driven piston (E) hits a lever arm which is rigidly attached to the outer cylinder. This kick induces an impulse, which propagates inward, and moves the inner cylinder.

The laser-beam apparatus shown in figures 1 and 3 is the heart of the instrument. Light from the laser is split into two beams by a variable-density beam splitter. One beam hits a mirror attached to the inner cylinder, the other hits a mirror on the outer cylinder. Each beam is focused onto its own photodiode. Voltages generated by the irradiated photodiodes are detected by voltmeters. In addition, the photodiodes are connected to a digital counter and a dual-channel oscilloscope. When the outer cylinder moves, its laser beam is directed off the corresponding photodiode. This action causes the voltage to drop, triggers the oscilloscope, and starts the counter. When the inner cylinder moves, its laser beam is removed from the corresponding photodiode. This action stops the counter.

Transit times may be obtained from the counter or oscilloscope. The counter conveniently provides a number, while the oscilloscope provides two voltage versus time diagrams. To obtain a transit time from the oscilloscope, the time at which each cylinder moves must be known. Therefore, since the movement of the cylinders leads to a sudden drop in voltage, the times at which the voltages for each cylinder begin to drop must be found, and the difference computed. Typical oscilloscope traces are displayed in sketches in figures 4 and 5 and photographs in figures 6, 7 and 8.

Consider, for example, figure 6. On the left we see the signals just before the measurement when the voltage is constant, equal to about 1.9 V on the photodiode for the outer cylinder and about 1.7 V on the photodiode of the inner cylinder. Each square of the grid in this voltage versus time diagram is 2×10^{-3} s wide and 250×10^{-3} V high. The start of the rotation of the outer cylinder is indicated by a

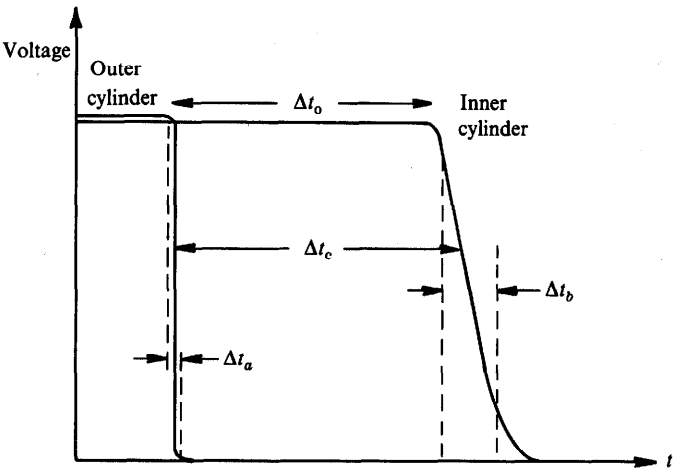

FIGURE 4. Sketch of voltage *vs.* time obtained from the oscilloscope for an elastic fluid in a small gap. Two different transit times Δt_o and Δt_c are measured on the oscilloscope and electronic counter respectively. The oscilloscope time Δt_o is the difference between the moment of onset of motion of the inner cylinder and the moment of onset of motion of the outer cylinder. Δt_c is measured with the counter and shown at the voltage level at which the counter is triggered. The fall times Δt_b and Δt_a for outer ($r = b$) and inner ($r = a$) cylinder are usually taken between 10 and 90 % of the initial voltage. The reader should note that the voltage *vs.* time graphs in figures 6–8 are digitized. The voltage drop corresponding to the outer cylinder consists of very few digital points and is difficult to distinguish.

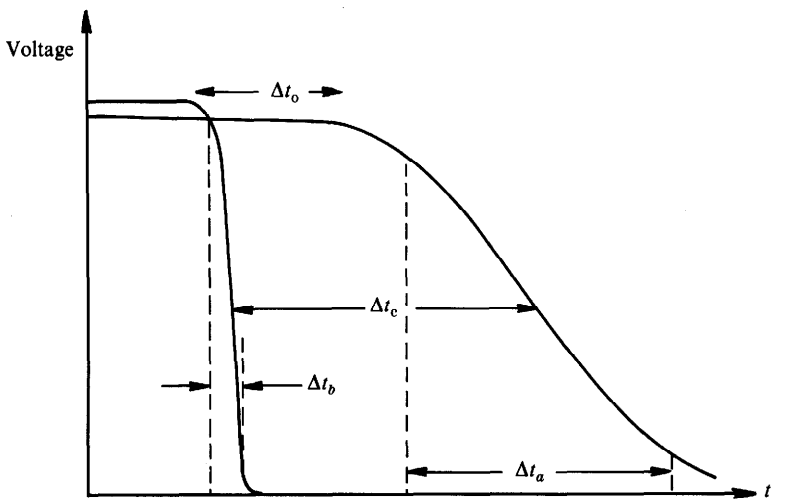

FIGURE 5. Sketch of voltage versus time for a more dilute solution in a large gap. The large fall time of the voltage at the outer cylinder, Δt_a, leads to a large difference in the transit times Δt_c and Δt_o measured on the counter and the oscilloscope.

sudden fall of the first signal along the dots, each 10^{-5} s apart. The motion can also be detected at the inner cylinder before the shear wave arrives. The signal at the inner cylinder becomes noisy when the outer cylinder is impacted. This noise is apparently due to vibrations of the metallic apparatus and perhaps to acoustic waves travelling through the liquid. These signals travel at speeds greater than 10^3 m/s and arrive after fractions of a μs. The noise is rapidly damped and the constant voltage at the

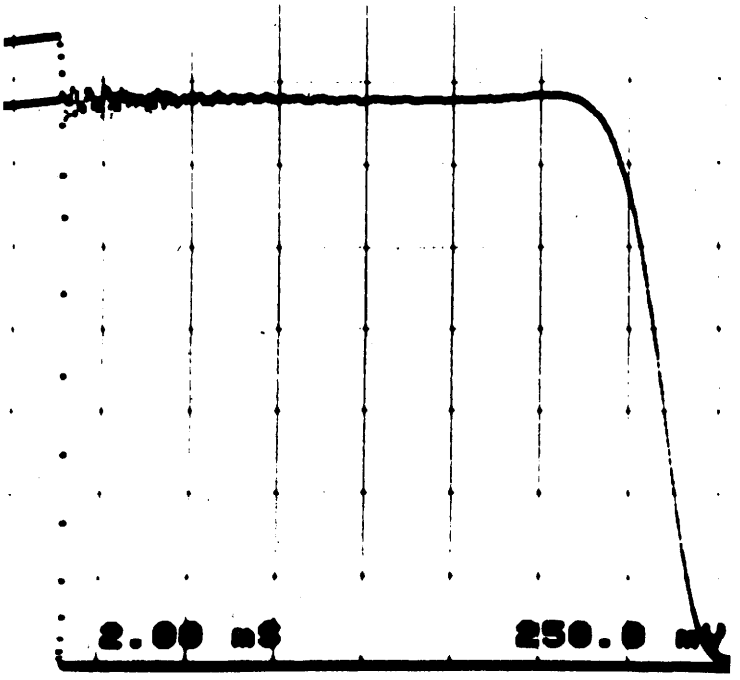

FIGURE 6. 1 % Polyox (coag.) in water; 2 mm gap; $\Delta t_c = 13.541$ ms; $c = 14.77$ cm/s.

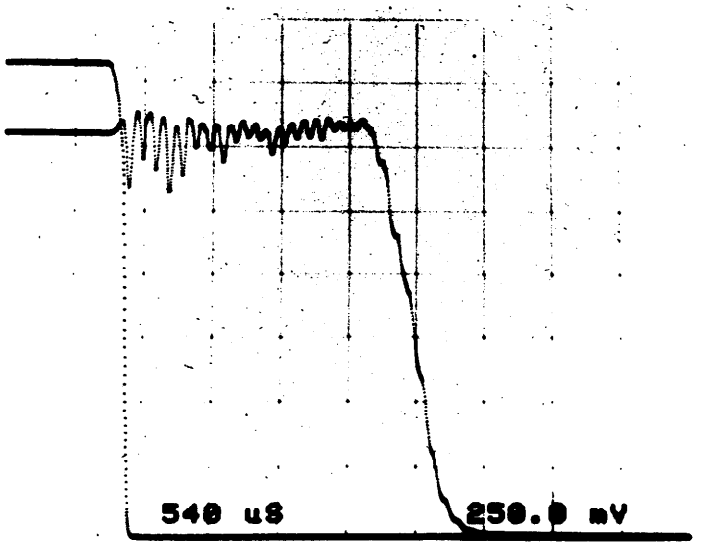

FIGURE 7. 1 % CMC in 50 % glycerin and 49 % water; 1 mm gap; $\Delta t_c = 2.218$ ms; $c = 45.09$ cm/s.

photodiode of the inner cylinder is restored. At a much later time, the transit time, the shear wave arrives and turns the inner cylinder. The oscilloscope shows this as a voltage drop.

Formulas for the angular velocity of the inner cylinder were developed in §§5 and 6 of Part 1 of this paper (Joseph, Narain & Riccius 1986*a*). The following considerations lead us to believe that the voltage drop as a function of time is linearly related to the angular displacement of the cylinders in the extremely small interval

FIGURE 8. Soybean oil; 3 mm gap; $\Delta t_c = 15.301$ ms; $c = 19.61$ cm/s.

of time it takes the laser beam to cross the photodiode. The d.c.-circuit containing the photodiode provides the voltage $V = RI$ to the oscilloscope, where R is the resistance and I the current. We operate the photodiode in a range in which I varies linearly with the light intensity as long as the intensity is not too small. The intensity changes as the laser beam sweeps across the photodiode. The circuit equation is

$$\frac{\mathrm{d}V}{\mathrm{d}t} = R\frac{\mathrm{d}I}{\mathrm{d}x}\frac{\mathrm{d}x}{\mathrm{d}t},$$

where $\mathrm{d}x/\mathrm{d}t = 2D\dot{\theta}$ and D is the distance between the mirrors and the photodiodes. $\mathrm{d}I/\mathrm{d}x$ is essentially constant over the small range of x covered by the laser light on the photodiode; hence

$$V(t) = K\theta(t), \quad K = 2RD\frac{\mathrm{d}I}{\mathrm{d}x}.$$

The diameter of the sensitive area of the photodiode is less than 1 mm; the diameter of the laser beam is about 1 mm and D is about 1.2 m.

The reading of the transit times from the oscilloscope involves an element of subjectivity through the evaluation of the voltage versus time diagrams. The counter, on the other hand, is triggered automatically when the signal falls from about 1.75 to 1.0 V. However, the counter time is less than the transit time read on the oscilloscope by as much as 50%. The oscilloscope times are closer to true transit times.

A comparison of figures 6, 7 and 8 shows that the drop of the signal for the inner cylinder is approximately parabolic in time and that the fall time increases with gap size. This dependence on time and gap size agrees with theoretical results derived in §6 of Part 1. The difference between transit times on the oscilloscope and the counter is exaggerated in larger gaps because the fall times are longer.

1.3. *Rise times and response times*

We use the term response time to mean the time taken by the instrument to register a wave after it has struck the inner cylinder. The rise time is the time taken for the outer cylinder to reach a constant velocity. The response time could be much smaller than the rise time.

We must first take note of the response time of the photodiode circuit and the oscilloscope. Since both of these are of $O(10^{-6}$ s), we cannot hope to measure anything that relaxes faster than 10^{-6} s on the meter as it is presently designed.

The rise time of our instrument is associated with the first reaction of the outer cylinder to an impulsive kick. This response represents a period of acceleration lasting from 30 to 100 μs. 30 μs is a typical time for the transfer of momentum between impacting elastic bodies. This period is followed by a rapid voltage drop of constant slope corresponding now to a constant angular speed of the outer cylinder. Typically the rise time is much smaller than the transit time. In this case the inner cylinder responds to a step increase in velocity. However, for very elastic fluids like the 600000 cs silicone oil in small gaps the transit and rise times can be of the same magnitude and the inner cylinder responds to somewhat smoother initial data.

We monitored the input signal with a high-speed video system (Spin Physics SP2000). The outer cylinder is still moving at nearly constant velocity after one transit time except in very dilute low-viscosity liquids in larger gaps. When the transit time exceeds 10 ms the outer cylinder comes to rest before a measurement is completed.

2. Criteria for shear waves

The criteria that we use to determine the existence of a shear wave and its speed are listed below. For a given fluid at a constant temperature we need to measure only one wave speed for different gap sizes. We define a *transit speed* by $c = d/\Delta t$, where Δt is the transit time. We say that c is a *shear-wave speed* if we get one value of c for different values of the gap size d. We think that our data show that for most fluids we have measured shear-wave speeds. The data are displayed so that readers may form their own opinion.

Given a shear-wave speed we define an experimental shear modulus

$$G_c = \rho c^2.$$

The degree of agreement between experimental shear moduli computed from wave speeds and independent measurements from step-strain and storage-modulus experiments is encouraging.

2.1. *Consistency checks*

We say that transit speeds are consistent with shear waves if the criteria listed below are satisfied.

(i) Repeatable transit times, without excessively large standard deviations, are measured. Averages and standard deviations are taken over about ten readings.

(iv) The transit time Δt is proportional to the gap size $b-a \overset{\text{def}}{=} d = c\Delta t$ with one and the same constant of proportionality c, independent of d. The reader can see which fluids pass these tests by reading the columns under c in tables 1 and 2. It is perhaps necessary to draw attention to the fact that we measured c for many d-values

in some liquids, and for few d-values in others. This is due either to the number of gap sizes that we had at a given time, to experimental problems in loading very viscous liquids into small gaps, to other experimental problems or because we were satisfied that nothing new would emerge from changing the gap size further.

(iii) The shear modulus $G_c = c^2\rho$ is consistent with stress relaxation for *all* liquids for which standard rheometers work. Practically, this means that

$$G_c > G(t)$$

for $t \geqslant t_0 > 0$, where $t_0 = 0.02$ s. This is the rise time on the Rheometrics System Four and the Rheometrics Fluid Rheometer used in our experiments. It is also typical for other standard rheometers. In §4 we shall examine this consistency check in detail.

(iv) The shear modulus $G_c = c^2\rho$ is consistent with values of the storage modulus $\tilde{G}'(\omega)$ taken in independent measurements. The nature of this consistency requires a little thought and will be discussed in §§4 and 5.

(v) The dependence of the wave speed and the corresponding shear modulus on temperature, concentration and molecular weight follows trends set by established theories and experiments. This type of consistency check is discussed in §§3, 4 and 5.

We have gained confidence in the wave-speed meter through experience with its performance. It is hard to describe this rather elusive criterion except to say that we observed many instances of apparent inconsistency and all of them were evanescent.

2.2. *Sensitivity checks*

Some checks to determine the sensitivity of c on parameters of the apparatus are discussed below.

Large changes of the moment of inertia of the inner cylinder led to only small changes in the measured values of c. For example, a 42% change of the moment of inertia changed c by less than 2.3% in soybean oil (plus additives, sold under the brand name 'Crisco'). A more important observation is that different inner cylinders corresponding to different gap sizes have different moments of inertia but they give rise to the same wave speeds.

One of the nicer design features of the present apparatus is the large wetted surface on the inner cylinder. This feature allows us to neglect end effects. The large wetted surface also transmits a large torque. A change in the filling level L in the gap reduces this torque. Small changes of L have no apparent effect on c. We changed L in a 1.38 mm gap filled with soybean oil. The value of c(cm/s) in the full gap was 22.0 ± 0.9, in the gap filled to $\frac{3}{4}L$, $c = 20.6 \pm 0.9$ and in the gap filled to $\frac{1}{2}L$, $c = 18.6 \pm 1.3$.

We also investigated the influence of friction at the pivot bearings of the inner cylinder. The inner cylinder rotates very easily. It can be turned even by gentle blowing. We changed the load on the pivot bearing by adding an additional load of 641%. The measured c for soybean oil in a gap of 1 mm changed by only 4%. This suggests that static and dynamic friction are negligible.

We studied the sensitivity of our measurements to changes in the size of the initial impulse at the outer cylinder. The spring-loaded kicking device has five different kick sizes. In addition we may change the position of the kicker relative to the lever arm.

It is of interest to record the effect of these changes on the wave speed c for a vegetable oil which like olive oil might be supposed to be Newtonian. The transit speeds for this oil are independent of gap size over a decade; the soybean oil appears to exhibit stress relaxation and also has a non-zero storage modulus at a low frequency (see figure 19).

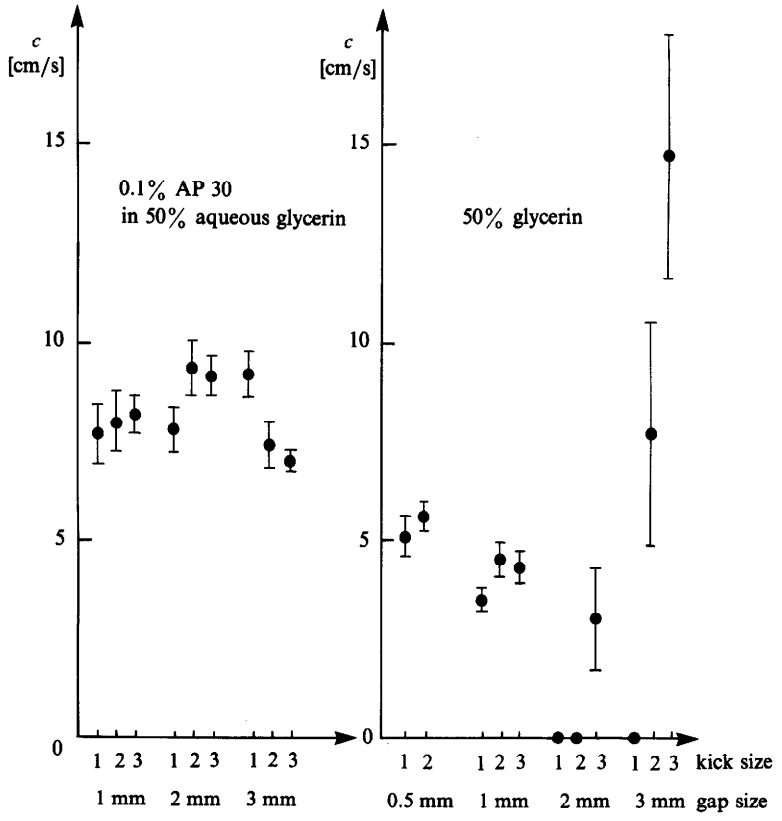

FIGURE 9. Variation of transit speeds with kick size in two liquids.

In figure 9 we display some of the results of tests with different kick sizes. We compare a very dilute and slightly elastic solution of 0.1 % poly(acrylamide) AP30 with its solvent (50 % aqueous glycerin). The measured wave speeds for the polymer solution stay in the same range for all gap and kick sizes, between 7 and 9.5 cm/s. The different kick sizes have only a small influence on c.

For the solvent 50 % aqueous glycerin we record a loss of the signal in the 2 mm gap. Only for kick size 3 is the signal strong enough to turn the inner cylinder. The measured wave speed, however, shows a strong standard deviation. This effect becomes even clearer when we examine the 3 mm gap. We observe again a loss of the signal for kick size 1. Both kick sizes 2 and 3 show large standard deviations and most importantly give very different values for c.

More-viscous fluids do not seem sensitive to changes in the size of the kick. For example, in 9.5 % PIB in decalin ($\tilde{\mu} = 139$ Pa s) we observed only a small change of the initial data for different kick sizes. The fall times of the input signal, which are related to the initial speed of the outer cylinder, correspond to the different kicks as follows: kick size 1 corresponds to a fall time of 98.4 μs, 2–104 μs, and 3–103 μs. In 10 % polystyrene ($MN = 22000$, $\tilde{\mu} = 0.011$ Pa s), however, kick size 1 corresponds to 110 μs, 2–99 μs, and 3–78 μs. Stronger kicks merely increase the elastic vibrations of the apparatus. More data on sensitivity checks can be found in Joseph, Riccius & Arney 1986*b*.

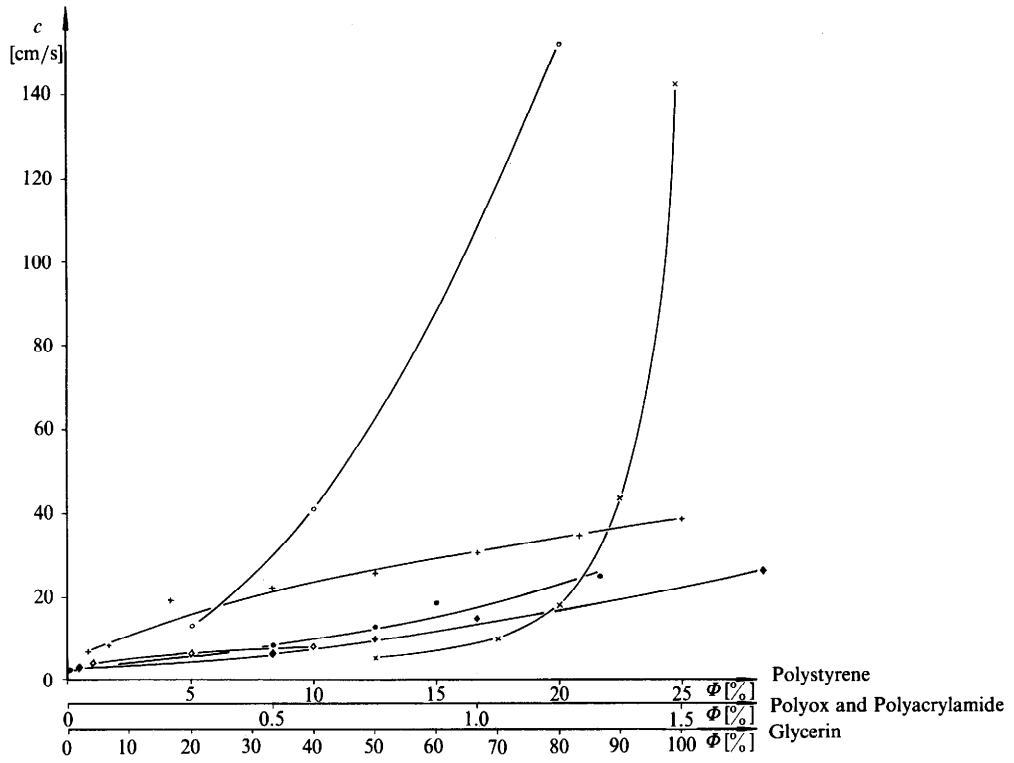

FIGURE 10. Wave speeds as a function of concentration. ○, polystyrene in decalin; $MN = 2$–3000000; ◇, polystyrene in decalin, $MN = 22000$; ●, Polyox (WSR-301) in water; ◆, Polyox (coag.) in water; ×, glycerin in water; +, polyacrylamide (AP 30) in 50% glycerin and $(50\text{-}\Phi)$% water.

2.3. *Brief summary of results*

We measured transit times in different liquids:

silicone oils of different molecular weight at different temperatures;
miscellaneous lubricating oils;
soybean oil, olive oil;
honey;
polymeric solutions in various degrees of dilution and molecular weight. Ten different polymers were used in solvents of water, water and glycerin, decalin, petroluem oil; and
aqueous glycerin in various degrees of dilution.

In general we get an elastic response for high-molecular-weight silicone oils and polymeric solutions that are not excessively dilute. All the fluids that have clear stress relaxation in the step-strain test and non-zero values of the storage modulus that increase with frequency pass all of our tests for shear-wave propagation. Many common 'Newtonian fluids' pass these tests; some common petroleum oils, soybean oil (Crisco), olive oil and glycerin. It is of course not surprising that these liquids are elastic but the wave speeds that we measure are orders of magnitude smaller than the wave speeds

$$c = O(G(0))^{\frac{1}{2}}, \quad G(0) = 10^{10}\ \text{dyn/cm}^2, \quad c = O(10^5\ \text{cm/s})$$

that are expected near the glassy state of full elasticity. Our instrument does not work for times shorter than 10^{-6} s and it cannot be expected to detect rapidly relaxing glassy modes. It is probable that our measurements of wave speed in these 'Newtonian liquids' reveal slower-relaxing structures than those associated with glassy states. Whatever the truth may be about the 'Newtonian liquids' they pass our criteria for elastic response unambiguously.

Other fluids which are even more 'Newtonian' give neither acceptable stress relaxation for the step-strain experiments nor non-zero storage moduli in sinusoidal oscillation experiments. These include water, dilute solutions of polymers in water, aqueous solutions of glycerin when the percentage of glycerin is less than 70 %, dilute solutions of polymers in aqueous glycerin, decalin, dilute solutions in decalin and low-viscosity silicone oils. The wave-speed data for these liquids are much more erratic. The standard deviations are large. The data (c or G_c) that we get in polymer solutions for decreasing concentration are perfectly normal, without anomalies, though anomalous data at extreme dilution is exactly what might be expected from 'Newtonian' solvents. To be clear about the last sentence, note that the wave speed c of aqueous Polyox (figure 10) passes smoothly to the measured value of c in pure water as the concentration is reduced to zero. Probably we pass smoothly from waves to diffusion as we reduce concentration. We see some evidence for this in the loss of signal at the larger gap sizes.

3. Wave speeds

Tables 1 and 2 presented in this section give all the values of c that we have measured up to October 1985. Measurements taken prior to May 1985 are summarized in table 1, those taken after May 1985 are summarized in table 2. All of the transit speeds in table 1 were measured on the electronic counter. After May we realized that the counter values of c could be as much as 50 % lower than oscilloscope values. In table 2 we give both the counter and oscilloscope data. The effective modulus G_c is obtained from the average $\bar{c}$ of c as $\overline{G}_c = \rho \bar{c}^2$. Gap sizes for various measurements of the transit speed are listed in mm.

The values of $\tilde{\mu}$, the static or zero-shear viscosity, were taken as limiting values of shear rate sweeps on a Rheometrics System Four rheometer, from a Rheometrics Fluid rheometer, or from published data.

We were not systematic in recording temperatures at the time of measurement prior to May 1985. These data, given in table 1, were taken at temperatures varying between 22° and 24 °C.

In general all the data for each different gap size were collected on the same day. Data under c that were collected on different days are marked with *. Some liquids change properties from day to day because of temperature variations, evaporation or chemical reactions.

Readers may wish to determine when c is independent of d for small d. This independence is fairly unambiguous in most cases. We note that rapid spatial decay is expected in fluids with short memories, e.g. Newtonian fluids, and the response will appear to be diffusive in the larger gaps. This manifests itself as a decrease of c with d. Such decreases are evident in aqueous glycerin solutions with even small amounts ($\geqslant 20$ %) of water, water, silicone oil, 5 % polystyrene in decalin, and decalin. We cannot conclude that these fluids are elastic. On the other hand, *all* fluids will appear to be diffusive when the gaps are sufficiently large (see §3 of Part 1). We require that c be independent of d for small d.

Fluid	$\tilde{\mu}$ (Pa s)	$\bar{c}$ (cm/s)	$\bar{G}_c$ (Pa)	Gap (mm)	c (cm/s)	ρ (g/cm^3)
1 % Carboxymethyl cellulose in 50 % glycerin and 49 % water $MN = 16000$	44.8	50.6	305	1 2 3	47.3 ± 2.5 51.4 ± 1.4 53.1 ± 1.5	1.19
Amoco gear lubricant no. 140	1.63	368	12500	1 2	384.3 ± 7.8 352.1 ± 10.0	0.924
Glycerin	0.69	142	2550	1 2 3	134.6 ± 8.3 148.9 ± 12.0 143.3 ± 2.7	1.26
90/10 Gly/H_2O	0.15	43.5	233	1 2 3	46.7 ± 2.9 40.5 ± 1.7 43.4 ± 1.9	1.23
80/20 Gly/H_2O	0.04	18.1	39.3	0.25 0.5 1 2 3	18.3 ± 3.5 18.2 ± 1.3 17.8 ± 0.7 15.4 ± 0.6 12.2 ± 0.8	1.2
70/30 Gly/H_2O	0.03	9.7	11.1	0.25 0.5 1 2 3	9.63 ± 1.1* 9.78 ± 0.86* 9.6 ± 0.3 6.9 ± 0.2 6.6 ± 0.5	1.18
50/50 Gly/H_2O	0.01	4.7	2.5	0.25 0.5 1 2 3	4.67 ± 0.6 5.89 ± 0.24 3.5 ± 0.3 0 0	1.12
Honey	249	1350	256000	1 2 3	1671.3 ± 498.5 1403.1 ± 268.9 977.2 ± 175.5	1.40
SAE 30 motor oil	0.098	76.3	516.0	1 2 3	81.7 ± 15.4 68.3 ± 6.6* 78.9 ± 5.8*	0.886
1.5 % Poly(acrylamide) separan AP 30 in 50 % glycerin and 48.5 % water $MN = 4000000$	160	38.4	172	1 2 3	37.5 ± 1.2 38.4 ± 3.2* 39.3 ± 1.7	1.17
1.25 % AP 30	112	34.3	137	1 2 3	33.8 ± 1.8 33.3 ± 1.8 35.8 ± 1.2	1.17
1.0 % AP 30	53.8	30.7	109	1 2 3	29.0 ± 1.1 31.1 ± 1.9 32.0 ± 1.5	1.16
0.75 % AP 30	26.4	25.3	74.3	1 2 3	25.5 ± 1.6 24.7 ± 1.4 25.7 ± 1.4	1.16
0.50 % AP 30	10.5	22.0	55.9	1 2 3	23.5 ± 1.2 22.1 ± 1.2 20.4 ± 0.4	1.16
0.25 % AP 30	4.5	18.9	41.1	1 2 3	18.5 ± 1.2 18.0 ± 1.0 20.2 ± 2.2	1.15
0.10 % AP 30	0.3	8.3	7.6	1 2 3	7.7 ± 0.8 7.8 ± 0.6 9.3 ± 1.2	1.12
0.05 % AP 30	0.11	6.8	5.2	1 2 3	7.5 ± 0.7 6.1 ± 0.7 9.6 ± 3.3	1.13

TABLE 1. (*cont.*).

Fluid	$\bar{\mu}$ (Pa s)	$\bar{c}$ (cm/s)	$\bar{G}_c$ (Pa)	Gap (mm)	c (cm/s)	ρ (g/cm^3)
Poly(dimethyl siloxane) PDMS 60000 cs silicone oil $MN = 65000$ lot no. LL 110426	63.6	719	50300	1	686 ± 129	0.974
				2	748 ± 49	
				3	1277 ± 101*	
PDMS 1000 cs silicone oil $MN = 16500$ lot no. 093564	0.97	167	2690	1	167.9 ± 25.9	0.967
				2	164.1 ± 4.9	
				3	168.4 ± 18.3	
PDMS 20 cs silicone oil $MN = 1500$ lot no. 103243	0.02	10.1	9.68	0.25	11.0 ± 0.8	0.949
				0.38	11.2 ± 1.8	
				0.5	9.0 ± 1.1	
				1	9.2 ± 1.0	
1.7 % Poly(ethylene oxide) (Polyox) coagulant in water $MN = 4000000$	58.4	25.7	68.0	0.25	22.3 ± 2.8	1.03
				0.50	24.4 ± 2.5	
				1	27.0 ± 0.6*	
				2	28.9 ± 1.3*	
1.0 % Polyox coagulant in water	6.12	14.7	21.5	0.25	12.7 ± 1.7	0.997
				0.50	14.3 ± 1.4	
				1	14.5 ± 0.5	
				2	16.1 ± 4.8	
				3	16.0 ± 0.5	
0.75 % Polyox coagulant in water	0.37	9.8	9.55	0.38	9.8 ± 0.6	0.994
				0.5	9.8 ± 0.6*	
0.50 % Polyox coagulant in water	0.1	6.9	4.69	1	6.8 ± 0.2	0.999
				2	6.9 ± 0.3	
				3	6.9 ± 0.3	
0.25 % Polyox coagulant in water	0.03	3.35	1.12	0.25	3.22 ± 0.71	1.00
				0.5	3.34 ± 0.30	
				1	3.39 ± 0.32	
				2	3.42 ± 0.99	
				3	3.37 ± 1.71	
0.25 % Poly(isobutylene) in Poly(butene)	12.3	1250	139000	1	1580 ± 600	0.893
				2	995 ± 158	
				3	1170 ± 102	
STP	14.3	286	7050	1	277 ± 42	0.858
				2	279 ± 10	
				3	304 ± 9	
Soybean oil (plus additives, brand name 'Crisco')	0.046	19.9	36.5	0.25	19.2 ± 3.3	0.922
				0.38	18.4 ± 2.1	
				0.50	20.9 ± 2.3	
				1	21.2 ± 2.2	
				1.38	22.0 ± 0.9	
				2	17.8 ± 1.7	
				3	15.5 ± 1.1	
TLA 227	22.3	234	4840	1	211 ± 16	0.884
				2	246 ± 3	
				3	245 ± 6	
Water	0.001	1.28	0.16	0.25	1.35 ± 0.13	1.000
				0.38	1.36 ± 0.17	
				0.50	1.12 ± 0.07	
				1	0	

TABLE 1. Transit speeds and shear moduli for different liquids. Data taken prior to 5 May 1985. This table gives wave speeds taken from the electronic counter. The counter values are from 10 to 50 % too low (cf. counter and oscilloscope values, table 2).

* Denotes data collected on a different day from the other data for that gap size.

Fluid	$\tilde{\mu}$ (Pa s)	$\bar{c}$ (cm/s counter)	$\bar{c}$ (cm/s oscill.)	$\bar{G}_c$ (Pa counter)	$\bar{G}_c$ (Pa oscill.)	Gap (mm)	c (cm/s counter)	c (cm/s oscill.)	T (°C)	ρ (g/cm^3)
Decalin (Decahydronaphtalene)	0.003	2.67	5.22	0.63	2.41	0.25	2.97±0.25	6.07±0.93	27	0.883
						0.38	2.60±0.28	4.92±0.43	28	
						0.5	2.43±0.21	4.67±0.59	25	
2% B200 in Decalin (D-1)	10.0	26.3	38.7	60.6	131	0.25	23.3±3.2	40.0±5.1	28	0.876
							21.6±2.0	41.7±6.8	28	
						0.5	25.6±2.1	43.1±6.6	28	
						1	26.4±1.2	35.3±2.7	28*	
						2	29.7±0.9	35.9±2.2	29	
						3	31.2±0.6	36.0±1.3	30	
10% B50 in Decalin (D-2)	1.7	76.1	102.2	509	918	0.25	62.8±6.9	90.0±15.9	28	0.878
						0.5	70.3±6.6	110.1±23.5	28	
						1	72.2±4.7	94.2±10.6	28	
							67.3±4.6	86.9±6.8	30*	
						2	86.1±7.4	109.6±12.0	26*	
						3	89.2±5.5	107.3±8.4	26*	
9.8% Elvacite in DEM	0.71	42.6	67.7	199	503	0.25	32.9±3.8	66.8±12.6	26	1.100
						3	52.2±4.8	68.5±6.7	25*	
Glycerin	0.69	145	196	2630	4840	0.25	360±41	219±19	24	1.255
						0.50	170±36	199±24	25	
						1	135±11	227±15	25	
						2	148±12	219±35	25	
						3	140±9	180±14	25	
						6.75	131±5	157±10	24	
Olive oil (Olio Sasso)	0.06	20.5	31.9	38.4	93.0	0.25	19.8±3.7	30.6±0.4	25	0.914
						0.50	22.4±1.8	33.9±5.0	25	
						1	24.2±1.5	40.1±5.1	26	
						2	19.0±1.0	30.7±2.2	26	
						3	17.1±1.0	24.0±0.8	26	
600000 cs Poly(dimethyl Siloxane) (PDMS) $MN = 110000$	586	1391	1471	189000	211000	3	1154±108	1270±217	24	0.977
						6.75	1627±73	1671±96	24	
100000 cs PDMS $MN = 75000$	98	1073	1372	112000	184000	1	1057±202	1320±381	23	0.977
						2	1179±86	1423±140	23	
						3	982±71	1373±136	23	

TABLE 2. (*cont.*)

Fluid	$\tilde{\mu}$ (Pa s)	$\bar{c}$ (cm/s counter)	$\bar{c}$ (cm/s oscill.)	$\bar{G}_c$ (Pa counter)	$\bar{G}_c$ (Pa oscill.)	Gap (mm)	c (cm/s counter)	c (cm/s oscill.)	T (°C)	ρ (g/cm³)
60000 cs PDMS $MN = 65000$	58	794	965	61400	90700	1.5	747±86	1018±136	24	0.974
						2.5	841±112	912±209	26	
12500 cs PDMS $MN = 41000$	12.2	540	598	28400	34900	1	501±58	490±22	25	0.975
						2	538±38	636±72	26	
						3	580±26	668±43	25	
12500 cs PDMS $MN = 41000$	25	547	613	29900	37500	2	547±65	613±55	0	0.999
	19.8	508	621	25500	38100	2	508±71	621±25	10	0.989
	12.2	513	599	25700	34900	2	513±39	599±27	25	0.975
	6.6	428	494	17300	23000	2	428±19	494±17	59	0.942
	5.6	324	445	9800	18500	2	324±20	445±65	70	0.932
1000 cs PDMS $MN = 16500$	1.09	144	200	2000	3870	1	137±4	216±9	25	0.967
						2	138±7	170±12	25	
						3	156±13	214±28	25	
1000 cs PDMS $MN = 16500$	1.7	223	257	4950	6570	2	223±21	257±26	0	0.995
	1.2	191	241	3590	5710	2	191±7	241±28	12	0.983
	0.67	150	172	2190	2840	2	151±14	172±5	35	0.961
	0.57	120	176	1390	2940	2	121±8	176±9	48	0.949
20 cs PDMS $MN = 1500$	0.02	18.2	30.5	31.4	88.3	0.25	32.1±3.9	54.7±8.5	26	0.949
						0.5	13.4±1.1	24.0±3.5	25	
						1	9.07±0.66	12.7±1.74	25	
1.3% Poly(ethylene oxide) in water $MN = 3000000$ (Polyox, WSR-301)	11.9	18.9	24.7	35.6	60.8	0.5	17.1±0.6	24.8±1.7	25	0.999
						1	18.7±0.4	24.3±0.8	25	
						2	18.9±0.8	23.2±1.7	26	
						3	20.8±0.6	26.3±0.9	23	
0.9% Polyox, WSR-301	6.23	13.3	18.3	17.5	33.4	0.25	11.5±1.0	16.6±0.9	24	0.995
						0.5	13.1±0.5	19.1±1.5	25	
						1	13.1±0.2	17.8±1.1	25	
						2	14.6±0.4	20.9±1.0	25	
						3	14.1±0.4	17.2±0.6	25	
0.75% Polyox, WSR-301	1.4	10.2	12.4	10.3	15.4	1	9.2±0.7	11.6±1.0	23	1.000
						2	10.4±0.6	13.2±1.1	23*	
						3	10.9±0.2	12.4±0.6	23*	
0.50% Polyox, WSR-301	0.14	6.39	8.33	4.07	6.91	1	6.66±0.40	——	23	0.997
						2	6.63±0.86	9.63±1.38	23	
						3	5.87±0.27	7.02±0.61	23	

TABLE 2. (*cont.*)

Fluid	$\tilde{\mu}$ (Pa s)	$\bar{c}$ (cm/s counter)	$\bar{c}$ (cm/s oscill.)	$\bar{G}_c$ (Pa counter)	$\bar{G}_c$ (Pa oscill.)	Gap (mm)	c (cm/s counter)	c (cm/s oscill.)	T (°C)	ρ (g/cm^3)
50 *P.P.M.* Polyox, WSR-301	0.0012	1.41	2.48	0.20	0.62	0.25	1.40±0.15	2.40±0.62	25	1.00
						0.38	1.45±0.12	2.44±0.33	25	
						0.5	1.38±0.34	2.59±1.44	25	
3% Poly(ethylene oxide) in water $MN = 4000000$ (Polyox coagulant)	181	59.8	71.7	347	499	2	55.9±1.4	71.7±1.0	28	0.97
						3	63.6±1.8	71.6±3.2	25	
9.5% Poly(isobutylene) in Decalin (Vistanex L-100) $MN = 1000000$	139	137	162	1570	2210	1	118±6	157±3	25	0.84
						2	150±3	179±6	26	
						3	142±4	151±15	25	
10% Poly(styrene) $MN = 22000$ in decalin	0.011	4.76	7.74	2.02	5.53	0.25	4.90±0.41	7.39±1.35	29.5	0.890
						0.5	4.61±0.75	8.26±1.57	27.5	
						1	4.78±0.38	7.57±0.75	28	
5% Poly(styrene) in declain	0.004	2.83	6.87	0.71	4.18	0.25	3.13±0.32	11.29±3.27	27	0.885
						0.5	3.07±0.31	7.49±0.15	27	
						1	2.52±0.20	4.47±0.49	27	
						2	2.58±0.38	4.22±0.74	28	
1% Poly(styrene) in decalin	0.003	2.57	4.96	0.58	2.14	0.25	2.55±0.23	5.64±1.40	27	0.873
						0.5	2.59±0.17	4.27±0.44	27	
						1	1.85±0.23	3.55±0.79	26	
20% Poly(styrene) $MN = 2$–300000 in decalin	2.3	123	153	1370	2120	1	123±10	172±15	25	0.908
						2	120±7	139±10	25	
						3	125±6	146±4	26	
10% Poly(styrene) in decalin	0.087	24.7	41.0	54.9	151	0.25	24.4±2.4	39.4±5.6	25.5	0.900
						0.5	26.1±5.3	50.1±5.5	26	
						1	23.6±0.9	33.5±1.9	26	
5% Poly(styrene) in declain	0.015	8.38	12.97	6.22	14.9	0.25	8.87±0.77	18.07±4.19	27	0.885
						0.5	8.71±0.29	11.00±0.71	28	
						1	7.57±0.55	9.83±0.82	25	

TABLE 2. Transit speeds and shear moduli for different liquids. * Denotes data collected on a different day from the other data for that gap size

Fluid	Gap (mm)	$\frac{dG'_\mu(0)}{2cG_\mu(0)}$	$G'_\mu(0)$ (10^5 Pa/s)
1% CMC	1	−0.1	−0.2
	2	−3.3	−9.0
	3	−2.6	−4.1
1.5% AP 30	1	−2.2	−9.9
TLA 227	1	−2.2	−380
	2	−0.2	−29
	3	−1.7	−250
Soybean oil	1	−2.7	−1.6
	3	−4.4	−2.2
1.7% Polyox coag.	0.25	−0.5	−3.4
	1	−1.2	−1.0
1% Polyox coag.	2	−3.0	−0.2

TABLE 3. Order-of-magnitude determination of $G'_\mu(0)$ from oscilloscope traces

3.1. *Dependence of wave speeds on concentration*

We turn next to the dependence of the transit speed on concentration. Results for two aqueous Polyox solutions, for poly(acrylamide) in a 50/50 glycerin–water solution, for two solutions of poly(styrene) in decalin and for aqueous glycerin solutions may be read from tables 1 and 2 and figure 10. These graphs show normal, rather than anomalous behaviour in that the wave speed and thus the corresponding modulus is a decreasing function of the concentration. Anamolous behaviour would be associated with glassy modes with timescales of order 10^{-7} s or shorter. These fast modes decay too rapidly to be measured on the wave-speed meter. It seems improbable that our data for dilute solutions give wave speeds associated with relaxing elasticity of slowly decaying modes. However, we could not establish diffusion for these cases and we think it prudent to leave the question open.

3.2. *Remarks about the experimental determination of* $G'_\mu(0)$

The oscilloscope traces (see figures 6, 7 and 8) can be used to determine order-of-magnitude estimates of the exponent $(dG'_\mu(0))/(2cG_\mu(0))$, which appears in Part 1, equation (6.7), and is important as a measure of decay of amplitude at the wavefront.

We find values of the exponent by evaluating the parabolic voltage drop representing the motion of the inner cylinder for small times $t-d/c$. An estimate of its order of magnitude is a different type of consistency check for our instrument, yielding two bits of useful information. The exponent gives the decay of the wave amplitude which must be large enough to detect the wave. For consistency we need very large, but finite values of $|G'_\mu(0)|$. We require that it should be possible to connect the point $G_c = G_\mu(0)$ with the measured relaxation function $G(s)$ (see the tangent construction given in figure 1, Part 1). In general this will require very steep slopes (see figures 11–16). At the same time the value of the exponent which contains $G'_\mu(0)$ as a factor should not be too negative. These two requirements, which at first thought are contradictory, are actually satisfied by our data (see table 3). We compute the parabolic trajectory from the oscilloscope trace. We have first to identify the vertex of the parabola. This identification is not accurate, especially when the gaps are small and the signals have small sinusoidal oscillations.

4. Comparison with independent measurements

As far as we know the wave-speed meter is the only instrument of its kind. It is based on the measurement of speeds of shear waves into a fluid at rest, rather than on measurements of stresses. The instrument has strong and weak points which we can assess by comparing it with other kinds of rheometrical experiments. The main comparisons will be made (i) with data on the stress relaxation function for different liquids taken on a standard cone-and-plate rheometer and (ii) with data on the storage modulus taken at different frequencies with different rheometers using small-amplitude sinusoidal oscillations.

Before starting on these comparisons we take note of the experiments of Lieb (1975) who uses tracer particles for flow visualization of shear waves in four fluids. He shows photographs indicating shear-wave propagation in only one of them, a solution of carboxymethyl-cellulose (CMC) in 49% water and 50% glycerin. He estimates $c > 8$ cm/s. We measure a shear-wave speed of $c = 50.6$ cm/s on the electronic counter (see table 1).

All of the following comparisons are indirect in that they are based on the computed value $G_c = \rho c^2$ of the shear modulus.

4.1. *Comparison with stress relaxation*

The simplified theory of stress relaxation (see, for example, Bird, Armstrong & Hassager 1977) is the underpinning for measuring relaxation in current state-of-the-art cone-and-plate rheometers. The stress-relaxation data in this report were taken on a System Four rheometer (Rheometrics, Inc., Union, NJ). Some details of design and use of this rheometer are discussed in the paper by Papanastasiou, Scriven & Macosko (1983). They note that

> Though in principle the relaxation modulus, ..., could be found from sufficiently small strains, ..., this is not entirely possible in practice for two reasons. The rise time of the instrument in step shearing is about 5 ms. Thus, $G(t)$ results are limited to $t > 0.01$ s. At times long enough that the torque on the transducer falls below 1 g_f cm the inherent noise and perhaps drift in the transducers (2000 g_f cm model) shows up as extraneous oscillation and deviations in the recorded curve.

The Rheometrics System Four, and other state-of-the-art rheometers do not work for thin liquids because the torque on the transducer is too small. Of course, there are borderline fluids of low viscosity, say about 10 P or so, for which the measured torques are barely high enough for the transducer. We regard our results for these fluids as uncertain. These types of rheometers appear to work fairly well for thicker, less 'Newtonian' fluids, such as 9.5% Vistanex L-100 in decalin.

We recall now that η, the elastic viscosity, is the area under the relaxation curve and the static viscosity $\tilde{\mu}$ is not smaller than the elastic viscosity, $\tilde{\mu} \geqslant \eta$. Nearly all the area under the relaxation curve of fluids with short-range memory is in the region of small times $s > 0$. Since $G(s) \approx 0$ for large s, the large-s values are not important for liquids with short-range memory. Since $G(s)$ is unknown for small $s > 0, s \neq 0$, the area under the relaxation curve cannot be computed for liquids with short-range memory. The area under relaxation curves for fluids with long-range memory depends strongly on the values $G(s)$ for large s. These long-range-memory values are also not computable from data taken on the Rheometrics System Four. The value $\tilde{\mu}$ of the static viscosity is shown on the figures as the area of a square of side $\tilde{\mu}^{\frac{1}{2}}$.

In the data given here we get $G(t)$ when $t \geqslant 0.02$ s, when the torque on the

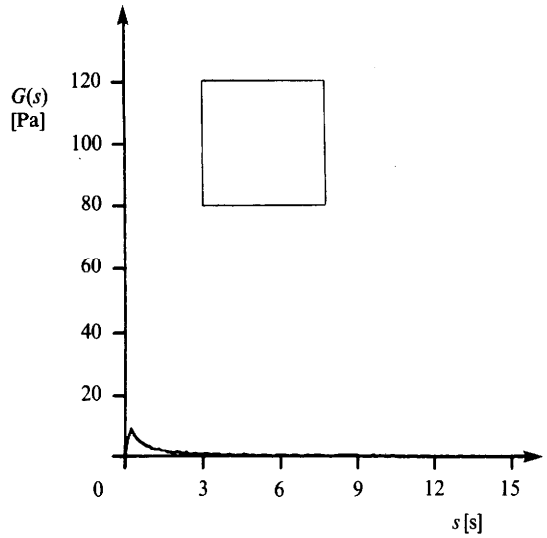

FIGURE 11. Shear modulus $\overline{G}_e = 256000$ Pa and relaxation function for honey, ($T = 32$ °C, $\gamma = 1$). The zero-shear viscosity $\tilde{\mu} = 196$ Pa s ($T = 32$ °C) is the area of the square.

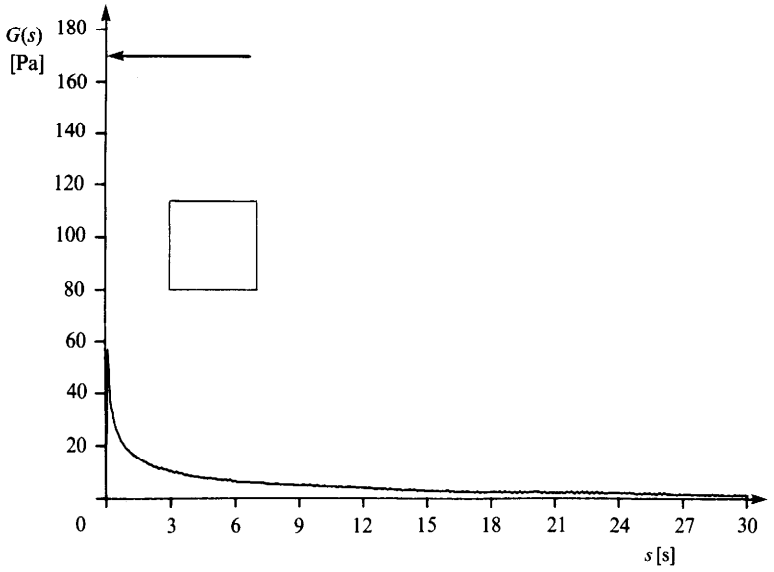

FIGURE 12. Shear modulus $\overline{G}_e = 172$ Pa and relaxation function $G(s)$ for 1.5% poly(acrylamide) Separan AP 30, 50% glycerin and 49% water, MN = 4000000 ($T = 30$ °C, $\gamma = 1$). The zero-shear viscosity $\tilde{\mu} = 160$ Pa s ($T = 30$ °C) is the area of the square.

transducer is above the critical 1 g_f cm value. Since we are at the border of this critical condition in many liquids, a certain degree of caution in interpreting the data is advisable. The first high rise in the graphs of stress relaxation shown here satisfies the required condition on the torque on the transducer.

The values of the strain γ in the step-strain experiment are indicated on the figures 11–16. For linear theories, the smaller the value of the strain, the better. We could not satisfy the critical condition for the torque with small strains in many fluids. By

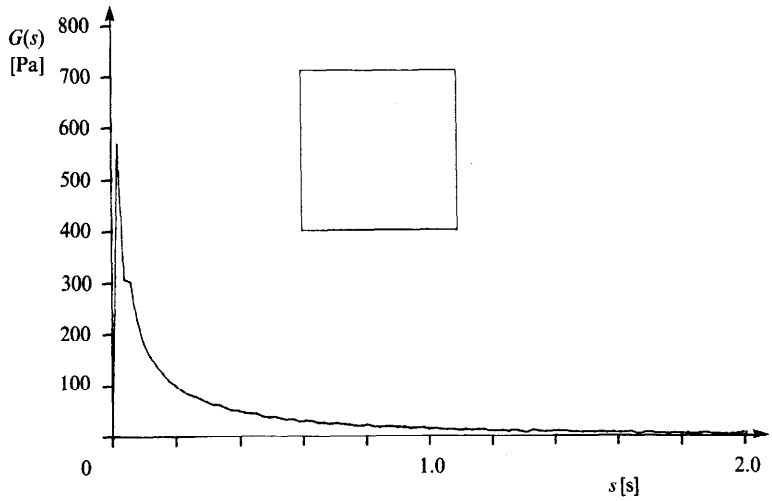

FIGURE 13. Shear modulus $\overline{G}_c = 2210$ Pa and relaxation function $G(s)$ for 9.5 % poly(isobutylene) (Vistanex L-100) in decalin, $MN = 1000000$, ($T = 25$ °C, $\alpha = 1$). The zero-shear viscosity $\tilde{\mu} = 139$ Pa s ($T = 25$ °C) is the area of the square.

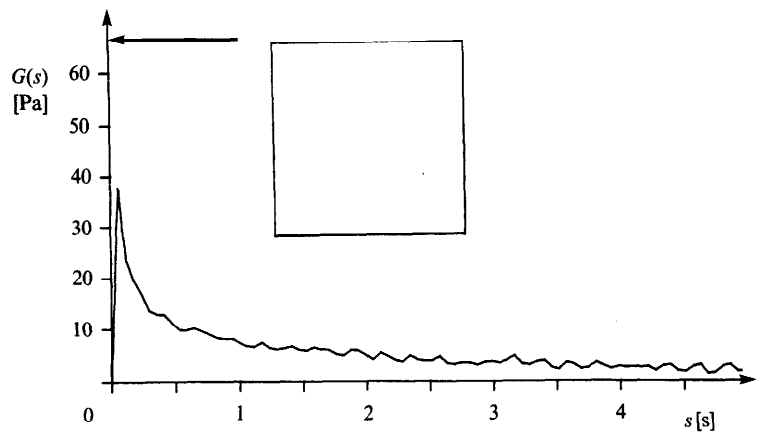

FIGURE 14. Shear modulus $\overline{G}_c = 68.0$ Pa and relaxation function $G(s)$ for 1.7 % polyox coagulant, $MN = 4000000$, ($T = 28$ °C, $\gamma = 1$). The zero-shear viscosity $\tilde{\mu} = 58.4$ Pa s ($T = 27$ °C) is the area of the square.

and large we went to the smallest strains for which we could get reliable readings. The graphs of $G(t)$ do depend on the strain.

On each figure we give the mean value of the shear modulus $\overline{G}_c = \rho\overline{c}^2$ that was measured on the wave-speed meter. We should remind the reader that values of $\overline{G}_c$ taken from table 1 are based on counter rather than oscilloscope values and are therefore too low. Despite this $\overline{G}_c$ is larger, usually much larger, than the largest value $G(t)$ recorded on the Rheometrics System Four. This indicates that we are getting $G(t)$ at early times $\epsilon \leqslant 0.02$ s, at least. In the next two sections we shall compare our wave-speed data with data from dynamic measurements. This comparison suggests that $\epsilon < 0.001$ s may be a conservative estimate of the time ϵ of response, $G_c = G(\epsilon)$.

Figures 11–16 and table 4 should be studied together. These figures and that table are arranged according to decreasing viscosity. There is no correlation between

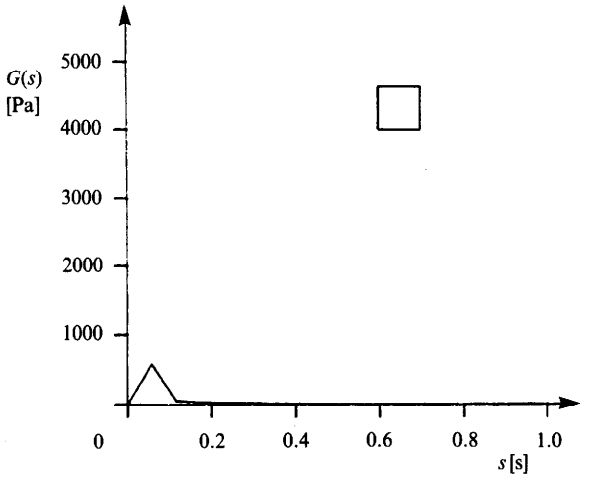

FIGURE 15. Shear modulus $\overline{G}_c = 90700$ Pa and relaxation function $G(s)$ for 60000 cs PDMS, $MN = 65000$, ($T = 24$ °C, $\gamma = 1$). The zero-shear viscosity $\tilde{\mu} = 58$ Pa s ($T = 24$ °C) is the area of the square.

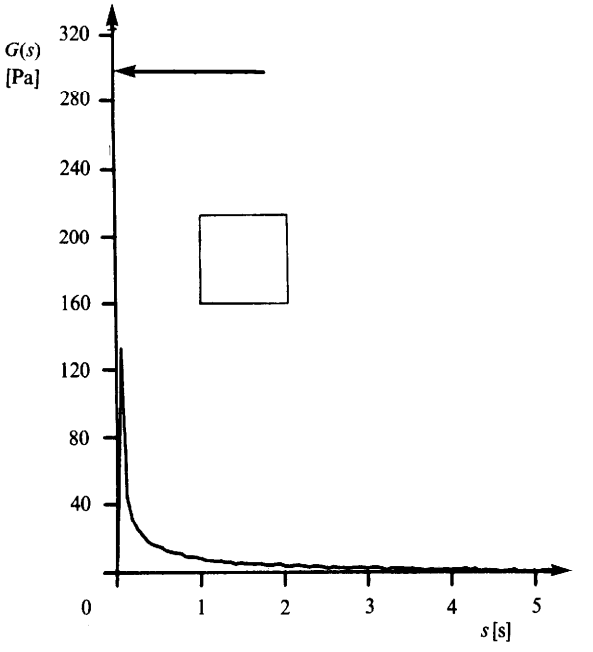

FIGURE 16. Shear modulus $\overline{G}_c = 305$ Pa and relaxation function $G(s)$ for 1 % carboxymethyl cellulose in 50 % glycerin and 49 % water, $MN = 160000$ ($T = 23$ °C, $\gamma = 1$). The zero-shear viscosity $\tilde{\mu} = 53.4$ Pa s ($T = 23$ °C) is the area of the square.

viscosity and rigidity. However, the ratio $\tilde{\mu}/G_c$ can be regarded as a mean relaxation time for the effective modes. Readers may verify that this mean relaxation time does describe in some sense just what one sees in figures 11–16.

There are 26 more such stress-relaxation plots for other liquids in Joseph *et al.* (1986*b*), which is available on request. All of our tests of stress relaxation were consistent with the measured wave speeds and figures 11–16 are representative.

4.2. *Comparison with dynamic measurements*

Dynamic measurements give the response of the liquid to small-amplitude sinusoidal oscillations of frequency ω. This type of measurement is the best diagnostic tool for determining the viscous and elastic response of liquids in the linear range (see §2 of Part 1). The elastic response in dynamic measurements is given by the storage modulus $\tilde{G}'(\omega)$. The limiting $\omega \to \infty$ value of the storage modulus is equal to the instantaneous value of the relaxation function (the rigidity), $\tilde{G}'(\infty) = G(0)$. Various techniques have been devised for determining $\tilde{G}'(\omega)$ for very large values of ω. If it were possible to determine $G(t)$ from $\tilde{G}'(\omega)$, we could use dynamic measurements to say something about the time of response ϵ at which $G(\epsilon) = G_c$.

It is customary to note that since both $G(t)$ and $\tilde{G}'(\omega)$ are measures of stored elastic energy a dynamic measurement at frequency ω is qualitatively equivalent to a transient at $t = 1/\omega$. This statement could be misinterpreted to mean that $\tilde{G}'(1/t)$ and $G(t)$ are close at small times. In fact, though they have the common value $G(0)$ at $t = 0$, the values separate at a 'maximum' rate because whereas

$$\frac{\mathrm{d}}{\mathrm{d}t}\tilde{G}'\left(\frac{1}{t}\right)\bigg|_{t=0} = -2G''(0)\,t + O(t^3)\bigg|_{t=0} = 0 \tag{4.1}$$

is stationary,

$$\frac{\mathrm{d}G(t)}{\mathrm{d}t}\bigg|_{t=0} \approx -\infty \tag{4.2}$$

is very large. For certain relaxation functions, $\tilde{G}'(1/t)$ and $G(t)$ can be very different, even at small values of t. For example, the ratio of the storage modulus to the relaxation function for a Maxwell model with a single relaxation time λ,

$$\frac{\tilde{G}'\left(\frac{1}{t}\right)}{G(t)} = \frac{\lambda^2/t^2}{1+\lambda^2/t^2}\exp\left(\frac{t}{\lambda}\right), \tag{4.3}$$

can be arbitrarily large, even for small t, if the relaxation time λ is sufficiently small. The reason for this is that the relaxation function decays exponentially while the storage modulus decays algebraically.

In figures 17 and 18 we have compared $G(t)$ and $\tilde{G}'(1/t)$ for

$$\left.\begin{aligned} G(t) = \sum_{n=0}^{25} G_n \exp\left(\frac{t}{-\lambda_n}\right), \quad \tilde{G}'\left(\frac{1}{t}\right) = \sum_{n=0}^{25} G_n \frac{\lambda_n^2/t^2}{1+\lambda_n^2/t^2}, \\ (G_0, G_1, G_n) = \left(10^9, 10^4, 10^4 \Big/ \sum_{n=1}^{25} n^{-3}\right), \\ (\lambda_0, \lambda_1, \lambda_n) = (10^{-8}, 3\times 10^{-3}, 3\times 10^{-3}/n^3). \end{aligned}\right\} \tag{4.4}$$

This relaxation function has one fast and 25 slow modes. It is representative for relaxation functions with widely separated spectra. The purpose of this comparison is to show that an effective modulus $G_\mu(0)$ could be masked in the storage modulus by the slow algebraic decay of the fast mode. The dramatic differences shown in figure 17 are reduced in regions in which $G(t)$ is slowly varying.

In general, for relaxation functions that admit a spectral representation,

$$\tilde{G}'\left(\frac{1}{t}\right) \geqslant G(t), \tag{4.5}$$

with equality at $t = 0$ and $t = \infty$ (see Ferry 1980, pp. 41, 42 and 69). The inequality (4.5) allows us to compare wave-speed and storage-modulus measurements.

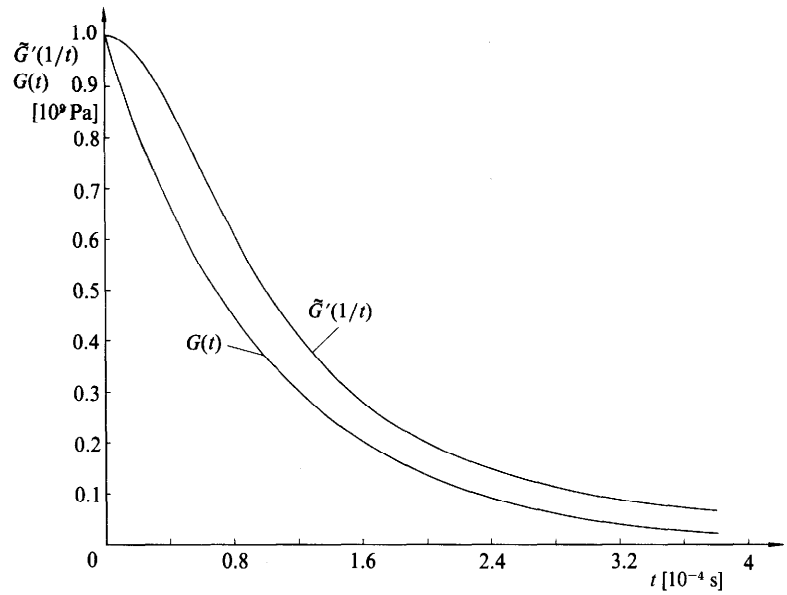

FIGURE 17. Comparison of relaxation function and storage modulus given by (4.4). This comparison is for short times on a linear scale. The comparison shows huge differences at early times.

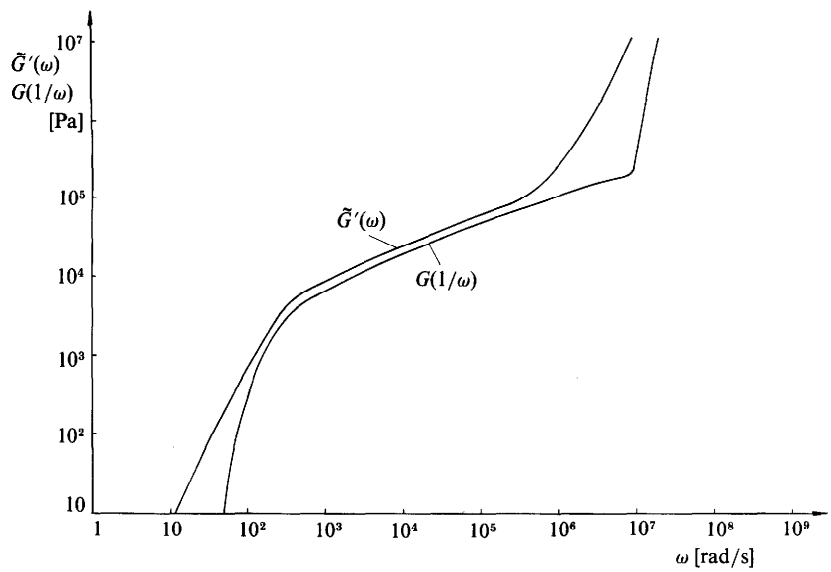

FIGURE 18. Comparison of relaxation function and storage modulus given by (4.4). This comparison is set in the logarithmic coordinates used by polymer chemists. The existence of an effective modulus $G_\mu(0) \approx O(10^5)$ is not so clearly evident in the storage modulus.

The storage modulus may be measured on most cone-and-plate rheometers. These rheometers are designed to work with very viscous liquids and are limited to a frequency range, below 1000 rad/s. We took these dynamic measurements on the Rheometrics System Four, with a maximum frequency of about 500 rad/s on the following liquids: soybean oil, olive oil, glycerin, aqueous Polyox in concentrations of 0.9 and 1.3 %, 10 % B50 in decalin, silicone oil of viscosity 10, 125, 1000 and 6000 St. In all cases G_c is substantially larger than the largest value $\tilde{G}'(\omega)$ for $\omega = 500$ rad/s. From this, and the inequality (4.5), we conclude that $G_c = G(\epsilon)$ with $\epsilon < 0.002$ s.

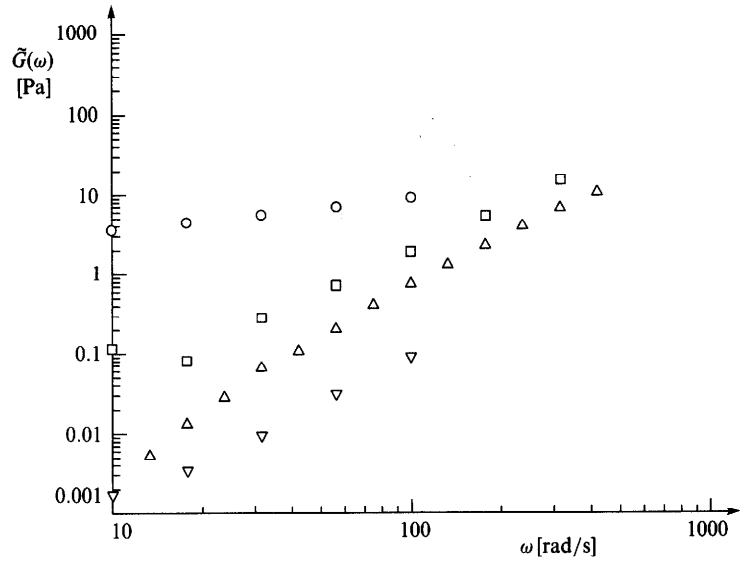

FIGURE 19. Storage modulus for different liquids. ○, 0.9 % Polyox, WSR-301; □, glycerin; △, olive oil; ▽, soybean oil.

The same type of comparison holds for some fluids on which independent data have been published. Values of the storage modulus for 2 % B200 in decalin for frequencies up to 80.8 rad/s are given by Walters (1983). The highest value of $\tilde{G}'$ is 31.1 Pa at the highest frequency and $G_c = 131$ Pa. Bird *et al.* (1977) exhibit data of Huppler, Ashare & Holmes (1967) for the storage modulus of a 1.5 % solution of poly(acrylamide) in 50 % glycerin and 48.5 % water. They say that $\tilde{G}'(\omega)$ is nearly at its limiting value with $\tilde{G}'(\omega) = 140$ Pa at frequencies of $\omega = 100$ rad/s. By a limiting value we understand an effective modulus. We measured a $G_c = 172$ Pa on the counter. The oscilloscope value would be much higher.

In figure 19 we present machine plots of dynamic data for 0.9 % aqueous Polyox, soybean oil, olive oil and glycerin. The last three liquids are commonly considered to be Newtonian. However, they appear to be elastic on the Rheometrics System Four (they pass the torque test for the transducer) and they give rise to a wave speed. We are reluctant to conclude that these fluids are elastic, and wish to let the readers draw their own conclusions.

5. Comparison with high-frequency data on silicone oils

In this section we shall compare data for the storage moduli of six different poly(dimethylsiloxane) liquids given by Barlow, Harrison & Lamb (1964, hereafter called BHL) with our data giving shear-wave speed and the corresponding shear modulus for some of the same liquids. BHL measured the shear mechanical impedance in silicone oils over a frequency range of 10 KHz–78 MHz at temperatures from $-50°$ to 50 °C on three different instruments. The complex rigidity can be obtained from the shear mechanical impedance. The comparison we wish to make can be read from figure 20. To understand this figure the reader should understand the method of reduced variables and how to compare the storage modulus $\tilde{G}'(\omega)$ with the relaxation function $G(1/\omega)$.

The method of reduced variables is widely used to compute master curves for the

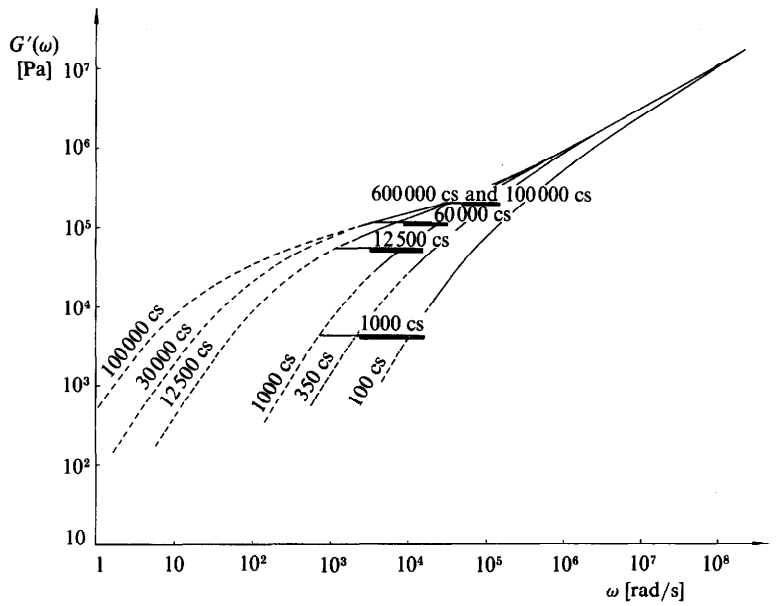

FIGURE 20. Storage modulus $\tilde{G}'(\omega)$ measured by Barlow, Harrison & Lamb (1964) for silicone oils of different viscosity: solid curves represent experimental values and dotted curves application of the Rouse theory. The horizontal lines represent the values G_e obtained with the wave-speed meter. The heavy bars give the probable range of values $t = 1/\omega$ in which $t = \epsilon$ where $G_c = G(\epsilon)$ (cf. figure 18).

storage modulus (see Ferry 1980, chap. 11). To illustrate this method we consider the storage modulus

$$\tilde{G}'(\omega) = \frac{G(0)\lambda^2\omega^2}{1+\lambda^2\omega^2}, \quad G(0) = \frac{\eta}{\lambda},$$

corresponding to a Maxwell model $G(s) = (\eta/\lambda)\,\mathrm{e}^{-s/\lambda}$. We define two temperature-dependent functions $\alpha = \alpha(T), \beta = \beta(T)$ and define $G = G(0)$ at temperature T and G_0 at temperature T_0, with the same convention for λ

$$G = \beta G_0, \quad \lambda = \alpha\lambda_0. \tag{5.1}$$

Solving for α, we get

$$\alpha = \frac{\lambda}{\lambda_0} = \frac{\eta}{\beta\eta_0}.$$

Moreover

$$\tilde{G}'(\omega) = \beta\tilde{G}'_0(\alpha\omega).$$

If $\alpha(T)$ and $\beta(T)$ are known, measurements of $\tilde{G}'(\omega)$ at different temperatures could be used to get $\tilde{G}'_0(\Omega)$ at the reference temperature T_0 and a different frequency $\Omega = \alpha\omega$, reducing the data to a master curve. One of the problems of the method of reduced variables is that (5.1) must also hold for every mode of relaxation, with only one pair of functions (α, β), when there are N modes of relaxation, as in equation (2.6) of Part 1.

There appears to be a certain agreement among persons doing high-frequency measurements, using the method of reduced variables, that the glassy modulus is only a weak function of temperature (see, for example, Harrison 1976). Some authors put $\beta = 1$ as an approximation. Then α is given by a viscosity ratio and α is large when T is small. In this case the effective frequency $\Omega = \alpha\omega$ of the storage modulus

at the reference temperature is large, and measurements of $\tilde{G}'(\omega)$ at small values of ω in a cold liquid give $\tilde{G}'_0(\Omega)$ in the liquid at the higher reference temperature T_0 and very high frequencies Ω.

The method of reduced variables is the only way presently known to obtain a master curve giving the storage modulus of a liquid at one temperature over the whole range of frequencies. In the literature one sees master curves which seem convincing; on the other hand, it is certainly not possible to say that this method works well in every situation (see Ferry 1980, p. 304–312) or completely in any situation. The data of BHL represented in figure 20 uses the method of reduced variables.

BHL studied six silicone oils manufactured by Midland Silicones Ltd with nominal viscosities $\tilde{\mu}$ and corresponding number-average molecular weights MN given by:

$\tilde{\mu}$ (cs)	100	350	1000	12500	30000	100000
$MN \times 10^{-4}$	0.63	1.58	2.1	4	5	6.8

Our silicone-oil samples were manufactured by Dow Chemicals:

$\tilde{\mu}$ (cs)	20	1000	12500	60000	100000	600000
$MN \times 10^{-4}$	0.15	1.65	4.1	6.5	7.5	11.0

The curves in figure 20 are due to BHL: the solid lines are meant to represent experimental values, the dotted lines represent an application due to BHL of the principles of the Rouse theory to silicone oils. BHL say that the results show clearly the existence of a plateau region in $\tilde{G}'$ (or $\tilde{G}''$, not shown here). The Rouse theory will not predict the existence of a plateau region. The vertical axis on figure 20 gives the storage modulus and the horizontal one gives the frequency ω in rad/s.

The horizontal bars in figure 20 represent our data in a manner which requires explanation. The horizontal bars are measured values of an effective shear modulus G_c. We are assuming that $G_c = G(\epsilon)$, where ϵ is the time of response. We do not know the value of ϵ at each measurement. In §4 we argued that $\epsilon < 0.002$ s. There is no precise way to relate our values of $G_c = G(\epsilon)$ to the values of $\tilde{G}'(\omega)$ of BHL other than to say, following (4.1), that

$$\tilde{G}'(\omega) \geqslant G\left(\frac{1}{\omega}\right), \quad \tilde{G}'\left(\frac{1}{\epsilon}\right) \geqslant G(\epsilon) = G_c.$$

If $\tilde{G}'(\omega)$ is a point on the experimental curve of BHL, then $G(1/\omega)$ lies below it. Since $\tilde{G}'(\infty) = G(0)$ there is another frequency $\Omega > \omega$ such that

$$\tilde{G}'(\omega) = G\left(\frac{1}{\Omega}\right) = G_c,$$

where, of course, $\epsilon = 1/\Omega$. We cannot find Ω exactly but it lies to the right of ω on the horizontal line $\tilde{G}'(\omega) = G_c$.

To make this comparison clearer we use the relaxation function for figure 18 which has a glassy mode, rubbery modes and an effective modulus. This example gives rise to a storage modulus which looks vaguely like the one given by BHL. We draw the reader's attention to the fact that the effective modulus, which is evident in the plot of $G(1/\omega)$, is masked by $\tilde{G}'(\omega)$. The reason for this is that $\tilde{G}'(\omega)$ decays only algebraically as ω is decreased (or t is increased). $G(1/\Omega)$ is already rubbery while $\tilde{G}'(\Omega)$ is still glassy.

We located the left-most point of the horizontal lines representing our data at the point $G_c = \tilde{G}'(\omega)$ by using the nominal viscosity as a parameter. We cannot

accurately compare our data with the data of BHL for the 20, 60000 and 600000 cs silicone oils not studied by them. We have indicated the probable location of our data for these oils in figure 20. The 60000 cs oil is neatly sandwiched between the 30000 and 100000 cs oils measured by BHL. The storage modulus for the 600000 cs oils probably has a more marked plateau than 100000 cs oil measured by BHL. The plateau values of the high-molecular-weight poly(dimethylsiloxane) liquids are evidently not sensitive to large viscosity differences (also, what is almost the same thing, large temperature differences). This feature is also characteristic of the values G_c measured in this study.

BHL attribute the existence of a plateau region to the formation of entanglement coupling in the silicone oils of high molecular weight. They find the molecular weights at which entanglement becomes important by looking for breaks in the slope of a viscosity versus molecular weight graph (their figure 9). The entanglements of long chains of macromolecules appears to become important for viscosities greater than a critical one in the range between 100 and 1000 cs.

All of our data points for silicone oils with viscosities larger than 1000 cs may be associated with plateau values of the shear relaxation function. This conclusion is further supported by data that we took at different temperatures. The value of G_c for the 600000 cs silicone oil does not appear to change strongly with temperature (see table 2). This suggests, through time–temperature superposition, that the corresponding storage modulus should be only weakly dependent on the frequency.

The data shown in figure 20 suggest that the wave-speed meter has a response time of the order $\epsilon = 1/\omega$, where $\omega = O(10^4)$. It may be possible, within the degree of rigour allowed by the empirical notion of reduced variables, to use supercooling to reduce the response time. To see how this might work we again use a simple Maxwell model

$$G(s, T) = G(T)\,\mathrm{e}^{-s/\lambda(T)}.$$

Then, using (5.1), we get

$$G(s, T) = \beta(T)\,G(T_0)\,\mathrm{e}^{-s/\alpha\lambda(T_0)} = \beta G\left[\frac{s}{\alpha}, T_0\right].$$

The reduced time s/α for supercooled liquids may actually enter into the region of small times needed to study the glassy response of liquids of low molecular weight.

6. Discussion

First, we gave a brief evaluation of the wave-speed meter. We developed a theory and experiment for measuring the speed of shear waves into rest. The speed of shear waves is independent of the distance travelled, for small distances. At larger distances the waves degenerate into diffusion. A shear modulus may be associated with a wave speed. This modulus is a value of the relaxation function at an early time.

As far as we know the wave-speed meter is the first rheological instrument based on measurements of the speed of shear waves into a fluid at rest rather than on measurements of stresses. The wave-speed meter is a short-time instrument for stress relaxation in the same sense that oscillating quartz crystals are high-frequency instruments for dynamic measurements which give storage and loss modulus. The main defect of the present design of the wave-speed meter is that we cannot measure the precise value of the short time ϵ at which the stress wave sensed by the instrument is generated. By comparing our experimental results with stress relaxation and the storage modulus, it appears that this early time may be of the order of 10^{-4} s.

We measured wave speeds for different liquids. Most of these, including many that might be thought to be Newtonian (lubricating oils, glycerin, olive oil, soybean oil) appear to be elastic at the short timescales of our machine. All of these liquids also exhibit elasticity in stress relaxation and have a non-zero storage modulus even at relatively low frequencies (500 rad/s) or large times (0.02 s) on the standard rheometers we used to check for consistency with our wave-speed measurements.

The wave-speed meter seems to be a more robust instrument than many other rheometers in current use. There are no major restrictions on viscosities or liquids that can be tested. The heat-control jacket that we use for controlling the temperature of our instrument allows us to measure wave speeds at temperatures between 0° to 70 °C. There seems to be no limitation, even in the present first-generation instrument, that would prevent one from measuring wave speeds with one instrument both in polymer melts and in supercooled liquids of low molecular weight.

The rheometrical data given by the wave-speed meter, wave speeds and effective rigidities cannot be obtained with other rheometers.

The second topic of this discussion addresses the scientific issues raised in this work. The concept of an effective viscosity and rigidity may be the most important one. This concept seems to be required to reconcile the common perception of elasticity in experiments on stress relaxation, dynamic measurement and wave speeds with the existence of a much faster glassy response. The glassy response is associated with enormous rigidities, 10^9 Pa, equally enormous rates of decay, say 10^{-8}–10^{-10} s, and wave speeds of the order 10^5 cm/s. The glassy response cannot be detected by any of the usual rheometrical instruments and it could not account for our perception of elasticity on the timescales of these instruments.

Effective rigidities are the rigidities one sees after the glassy modes have decayed. On slower, but possibly still enormously fast, timescales, the decayed glassy modes appear as an effective viscosity, without further dynamic consequences.

The notion of an effective rigidity is related to the notion of the spectrum of a liquid. A robust, more or less unique effective rigidity might be expected from a spectrum centred around two very different relaxation times. Such effective moduli have already been identified in pioneering experiments using high-frequency dynamic measurements on amorphous polymers. Mason *et al.* (1949) note that

> Both the torsional crystal and high frequency shear wave techniques applied to polyisobutylene and poly-α-methylstyrene liquids, show that there are two main relaxation frequencies in these liquids. At frequencies under 100 kc, the shear stiffness is in the order of 3×10^7 dynes/cm^2, while in the high megacycle range it has increased to 5×10^9 dynes/cm^2. The low shear elasticity appears to be associated with a composite motion of molecular rotation and translation that allows a configurational change to occur from the most probable chain shape. When the shear stress is removed, the molecule quickly returns to its most probable shape. This results in a low shear stiffness. At high frequencies this motion cannot take place, and the shear stiffness is determined by motions within single potential wells, and the value approaches that for a crystal.

We have explored the idea that values of G_c, which we measure in polymeric solutions of all degrees of dilution and in even in ordinary liquids, like soybean oil, are sufficiently robust and reproducible to be described as an effective rigidity. We have also showed that these effective rigidities could be masked in the algebraic decay of glassy modes on state-of-the-art high-frequency dynamic instruments measuring the storage modulus (cf. figure 18).

Fluid	$\tilde{\mu}$ (Pa s)	G_c (Pa)	$\tilde{\mu}/G_c$ (s)
Honey	193	256000	7.5×10^{-4}
AP 30 (1.5%)	160	172	9.3×10^{-1}
Vistanex	139	2210	6.3×10^{-2}
Polyox (1.7%)	58.4	67	8.7×10^{-1}
Silcone oil (60000 cs)	58	90700	6.4×10^{-4}
CMC (1%)	53.4	305	1.8×10^{-1}
Silcone oil (12500 cs)	12.2	34900	3.5×10^{-4}
B200 (2%)	9.5	131	7.3×10^{-2}
Glycerin	0.69	4700	1.5×10^{-4}
Polyox (0.5%)	0.1	6.9	1.4×10^{-2}
Olive oil	0.6	93	6.5×10^{-4}

TABLE 4. Summary of some experimental results (from tables 1 and 2) arranged according to decreasing viscosity $\tilde{\mu}$. The measured rigidity is $G = G_c$ and the mean relaxation time is $\tilde{\mu}/G$. Stress relaxation for the first two groups in this table is shown in figures 11–16

In reservation, we did not find strong support for the idea of a robust effective modulus, a value $G_\mu = G(\epsilon)$, relatively insensitive to changes in ϵ, in the literature on dynamic measurements. The idea of a plateau modulus does appear in this literature, usually for amorphous polymers with entanglement couplings. We do not mean to identify effective moduli, which we have also associated even with not particularly dilute polymeric solutions, with plateau moduli.

It is perhaps desirable to terminate our discussion of effective moduli with some remarks about Newtonian liquids. We have argued that the Newtonian viscosity could be defined in terms of remnants of modes already relaxed. This view gives a certain operational rather than fundamental significance to the Newtonian viscosity. In fact, a unique, effective (Newtonian) viscosity could be expected only in cases where the spectrum of the liquid is neatly separated so that fast and slow modes can be identified. The existence of such separated spectra is an open problem in the theory of liquids.

If we admit to fast modes and suppose that they give rise to a relatively small viscosity, we may put aside their smoothing effects and think, like Maxwell, about the rigidity G_c and time of relaxation $\tilde{\mu}/G_c$ of a liquid. Maxwell thought that viscous liquids were actually elastic ones with high rigidities and fast times of relaxation. He introduced (1873) birefringence to study the elasticity of liquids. He says that

> I have enumerated these instances of the application of polarized light to the study of the structure of solid bodies as suggestions with respect to the application of the same method to liquids so as to determine whether a given liquid differs from a solid in having a very small 'rigidity', but a sensible 'time of relaxation', or in both ways. Those which, like Canada balsam, act strongly on polarized light, have probably a small 'rigidity', but a sensible 'time of relaxation'. Those which do not show this action are probably much more 'rigid', and owe their fluidity to the smallness of their 'time of relaxation'.

Maxwell's clear perceptions are marred by the notion of a single time of relaxation. This notion does not allow for different relaxation effects in which slow modes with small rigidities actually carry the larger viscosity.

In table 4 we have summarized some of our experimental results, organizing them

in four groups according to decreasing viscosity $\tilde{\mu}$. The measured rigidity is $G = G_e$ and the mean relaxation time is $\tilde{\mu}/G$. Of course, if the finite value of G in the table is allowed, then none of these liquids can be said to be Newtonian. We can only say that some liquids are more Newtonian than others. Liquids that, like olive oil, have a small time of relaxation and also a small viscosity could not exhibit elasticity for very long. On the other hand, liquids like honey, or even more, 600000 cs silicone oil, that have a small time of relaxation but a large viscosity can have a persistent elastic (and even nonlinear) response. The stress in such materials relaxes rapidly but much more relaxing is required because the area under the relaxation curve is so large. There are probably no Newtonian liquids with large viscosities.

We would like to acknowledge the invaluable advice and help of Professor Gordon S. Beavers with the experiment reported in this paper. We express our gratitude to Professor C. Macosko and Professor W. G. Miller for letting us use their rheometers. This work was supported by the Army Research Office (Mathematics) and the National Science Foundation (Fluid Mechanics). The work of M. Arney was supported in part by a fellowship from the Plastics Institute of America.

This paper is taken from a larger report (no. 7 of the Fluid Mechanics Laboratory of the Department of Aerospace Engineering and Mechanics, hereafter designated as FML no. 7). This report is available on request.

REFERENCES

Barlow, A. J., Harrison, G. & Lamb, J. 1964 Viscoelastic relaxation of polydimethyl-siloxane liquids. *Proc. R. Soc. Lond.* A **282**, 228–251.

Bird, R. B., Armstrong, B. & Hassager, O. 1977 *Dynamics of Polymeric Liquids*. Wiley.

Ferry, J. D. 1980 *Viscoelastic Properties of Polymers*. Wiley.

Harrison, G. 1976 *The Dynamic Properties of Supercooled Liquids*. Academic.

Huppler, J. D., Ashare, E. & Holmes, L. A. 1967 *Trans. Soc. Rheol.* **11**, 159.

Joseph, D. D., Narain, A. & Riccius, O. 1986*a* Shear-wave speeds and elastic moduli for different liquids, Part 1. Theory. *J. Fluid Mech.* **171**, 289–308.

Joseph, D. D., Riccius, O. & Arney, M. 1986*b* Shear wave speeds and elastic moduli for different liquids, Part II: Experiments. *Fluid Mechanics Laboratory Report* (FML no. 7). Department of Aerospace Engineering and Mechanics, University of Minnesota.

Lieb, E. H. 1975 Viscoelastic flow behavior in accelerating shear fields. Ph.D. thesis, University of Delaware.

Mason, W. P., Baker, W. O., McSkimin, H. J. & Heiss, J. H. 1949 Measurement of shear elasticity and viscosity of liquids at ultrasonic frequencies. *Phys. Rev.* **75**, 936–946.

Maxwell, J. C. 1873 On double refraction in a viscous fluid in motion. *Proc. R. Soc. Lond.* **22**, 46–47.

Papanastasiou, A. C., Scriven, L. E. & Macosko, C. H. 1983 An integral constitutive equation for mixed flows: viscoelastic characteristics. *J. Rheol.* **27**, 387–410.

Walters, K. 1983 *The Second-Normal-Stress Difference Project, IUPAC Macro 83, Bucharest, Romania, Plenary and Invited Lectures, Part 2*, pp. 227–237.